Geophys. J. Int. (1994) **118, 428-438**

The fracture criticality of crustal rocks

Stuart Crampin*

Department of Geology and Geophysics, University of Edinburgh, Grant Institute, West Mains Road, Edinburgh EH9 3JW, *UK*

Accepted 1994 March 17: received 1994 March 13, in original form 1993 November 23

Preface. It is a pleasure and a honour to be included in this issue commemorating the centenary of Robert Stoneley's birth. I was, I believe, the last of the small number of research students supervised by Stoneley, and it gives me great pleasure that most of my research has been, by chance, in a field he initiated—(azimuthal) seismic anisotropy. Bob Stoneley was one of the first seismologists to consider azimuthally anisotropic seismic waves (specifically surface waves) in cubic (Stoneley 1955) and orthorhombic symmetries (Stoneley 1963). Although, he considered these papers 'essentially as a development in the theory of elasticity', they were invaluable references to me when I first began to calculate surface waves in an anisotropic Earth. Bob would have been gently amused that a large part of the Earth is now recognized as having orthorhombic anisotropic symmetry.

SUMMARY

The shear-wave splitting observed along almost all shear-wave ray paths in the Earth's crust is interpreted as the effects of stress-aligned fluid-filled cracks, microcracks, and preferentially oriented pore space. Once away from the free surface, where open joints and fractures may lead to strong anisotropy of 10 per cent or greater, intact ostensibly unfractured crustal rock exhibits a limited range of shear-wave splitting from about 1.5 to 4.5 per cent differential shear-wave velocity anisotropy. Interpreting this velocity anisotropy as normalized crack densities, a factor of less than two in crack radius covers the range from the minimum 1.5 per cent anisotropy observed in intact rock to the 10 per cent observed in heavily cracked almost disaggregated near-surface rocks.

This narrow range of crack dimensions and the pronounced effect on rock cohesion suggests that there is a state of ***fracture criticality*** at some level of anisotropy between 4.5 and 10 per cent marking the boundary between essentially intact, and heavily fractured rock. When the level of fracture criticality is exceeded, cracking is so severe that there is a breakdown in shear strength, the likelihood of progressive fracturing and the dispersal of pore fluids through enhanced permeability. The range of normalized crack dimensions below fracture criticality is so small in intact rock, that any modification to the crack geometry by even minor changes of conditions or minor deformation (particularly in the presence of high pore-fluid pressures) may change rock from being essentially intact (below fracture criticality) to heavily fractured (above fracture criticality). This recognition of the essential compliance of most crustal rocks, and its effect on shear-wave splitting, has implications for monitoring changes in any conditions affecting the rock mass. These include monitoring changes in reservoir evolution during hydrocarbon production and enhanced oil recovery, and in monitoring changes before and after earthquakes, amongst others.

Key words: cracked rock, differential shear-wave anisotropy, fracture criticality, shear-wave splitting.

1 INTRODUCTION

Shear-wave splitting, implying some form of effective elastic anisotropy, has been observed along almost all suitable shear-wave ray paths in at least the uppermost half of the Earth's crust. Such splitting is routinely observed in the shear-wave window above small earthquakes in a very wide range of igneous, metamorphic, and sedimentary rocks in a variety of tectonic regimes, and in reflection surveys, vertical seismic profiles (VSPs), reverse VSPs, and cross-hole surveys in seismic exploration of sedimentary

* Also at: Edinburgh Anisotropy Project, British Geological Survey, Murchison House, West Mains Road, Edinburgh EH9 3LA, UK.

basins. Kaneshima (1990) ad Crampin & Love11 (1991) are recent reviews of such observations. The splitting typically displays remarkably similar characteristics despite the wide range of geological and tectonic terrains in which the shear waves propagate. These similarities indicate a common origin of the splitting in the stress-aligned fluid-filled cracks, microcracks, and preferentially oriented pore space present in most rocks. Note that this paper refers to azimuthal anisotropy, where the polarizations of shear-wave splitting vary with azimuth. I do not consider here azimuthal isotropy (transverse isotropy) with a vertical symmetry axis where shear waves invariably split into *SV*- and W-wave orientations that may indicate merely that the crust is horizontally layered.

Two characteristics are critical for identifying distributions of cracks (fractures) as the origin of the azimuthal splitting:

(1) the horizontal projections of the polarizations of the leading split shear waves are usually parallel or subparallel for all ray paths within the shear-wave window (Crampin & Love11 1991; see also Booth & Crampin 1985 for a discussion of the shear-wave window).

(2) This direction is subparallel to the local direction of maximum horizontal compressional stress in rock volumes where orientations of both polarizations and stress have been reliably determined (Crampin & Evans 1986; Crampin & Love11 1991).

These characteristics are critical because first, the only anisotropic structure with a large enough solid angle of parallel polarizations at the surface (aperture greater than 70") is transverse isotropy (hexagonal anisotropic symmetry), or a minor perturbation thereof, oriented so that the symmetry axis is horizontal or subhorizontal (Crampin 1981). Secondly, parallel vertical cracks are the only phenomenon common to all types of crustal rocks that possesses transverse isotropy with a horizontal symmetry axis.

Hydraulic fracturing in the oil industry demonstrates that fluid-filled cracks are usually vertical and strike parallel to the maximum horizontal stress (or strictly, perpendicular to the minimum horizontal stress). In some cases, shear-wave splitting can be plausibly correlated with the presence of large fluid-filled fractures in sedimentary rocks, both directly (Mueller 1991; Lewis, Davis & Vuillermoz 1991), and indirectly (Cliet *et al.* 1991; Li, Mueller & Crampin 1993). Shear-wave splitting in igneous and metamorphic rocks appears to be the result of cracks and microcracks with diameters less than a few centimetres, possibly much less (Holmes, Crampin & Young 1993). There are also detailed correlations of VSPs with borehole data confirming that shear-wave splitting is associated with aligned cracks (Queen & Rizer 1990; Lefeuvre *et al.* 1993).

Other important phenomena indicative of cracks are temporal variations in the behaviour of shear-wave splitting before and after earthquakes (Booth *et al.* 1990; Crampin *et al.* 1990, 1991; Liu *et al.* 1993c), and before and after hydraulic pumping (Crampin & Booth 1989). Temporal variations in shear-wave splitting are expected during hydrocarbon production and enhanced oil-recovery operations, but have not yet been reported, although changes in the behaviour of *P* waves have been noted (Greaves & Fulp 1987; Bregman 1989; De Buyl 1989; Robertson 1989; and now many others). The only possibility of such temporal changes to the effective elastic parameters governing wave propagation in rock at comparatively low temperatures and pressures .is by changes to the internal geometry and pore fluids of the fluid-filled cracks, microcracks, and pore space within the rock mass.

This paper relates the degree of splitting with the crack density of the equivalent 3-D distribution of cracks. Since, the crack density varies as the cube of the normalized (average) crack radius, the range of normalized crack radii for the limited range of observed anisotropy is surprisingly small. The observed levels of anisotropy suggest that most ostensibly intact rocks in the crust are in a state close to *fracture criticality* (Crampin & Leary 1993). The crack density at fracture criticality marks the boundary between what may be considered as essentially intact unfractured rock and rock that is heavily fractured. Above fracture criticality, cracking is so pervasive that there is the loss of much shear strength, the comparatively free movement of fluids with enhanced permeability, and the likelihood of through-going fractures. Cracking and proximity to fracture criticality is indicated throughout most rocks, and has implications for monitoring temporal changes in the rock mass during hydrocarbon production, and in earthquake preparation zones, amongst others.

Note that in this paper, I do not distinguish between cracks and fractures, and use either term as convenient.

2 DIFFERENTIAL SHEAR-WAVE ANISOTROPY IN THE CRUST

Shear-wave splitting in crustal rocks, implying some form of seismic azimuthal anisotropy, was first observed above small earthquakes (Crampin *et al.* 1980b), but has now been widely observed in controlled-source reflection surveys (Alford 1986), VSPs (Crampin *et al.* 1986), cross-hole surveys (Liu, Crampin & Queen 1991), and reverse VSPs (Liu *et al.* 1993a). Occasionally shear-wave splitting may be plausibly attributed to phenomena other than cracks, such as rock foliation (Lüschen *et al.* 1991), or crystal alignment, but typically the anisotropy appears to be the result of propagation though distributions of aligned cracks, microcracks, and preferentially oriented pore space known as *extensive-difatancy anisotropy*, or *EDA* (Crampin, Evans & Atkinson 1984; Crampin 1993b). Individual cracks in, what I shall term intact, rock without large fractures are referred to as *EDA cracks*, since their behaviour can be simulated by distributions of parallel microcracks, even though it is recognized that their individual geometry may include a wide range of aligned structures.

The interpretation of shear-wave splitting as crack-induced anisotropy is dependent on the formalism of Crampin (1978) and Hudson (1980, 1981), who developed expressions for the effective elastic constants of a cracked solid, where crack density is defined as $\varepsilon = Na^3/v$, N is the number of cracks of radius a in volume v (O'Connell & Budiansky 1974; Hudson 1980, 1981). These formulations assume that, for wavelengths much larger than the crack dimensions, the behaviour of weak distributions of aligned cracks can be modelled by an effective elastic medium with the anisotropic symmetry appropriate for the particular crack distribution. The techniques assume that the cracks

are aligned, small (much less than the seismic wavelength), thin (aspect ratios ≤ 0.1), circular, and isolated (unconnected to other cracks). The formulations appear to be mathematically valid for crack distributions with crack densities of up to about $\varepsilon = 0.1$, approximately 10 per cent shear-wave velocity anisotropy (Crampin 1984). With these restrictions, synthetic seismograms calculated through such models simulating cracked rock have been able to match observed three-component seismograms in considerable detail (Bush & Crampin 1991; Liu *et al.* 1991, 1993a; Slater *et* al. 1993; Yardley & Crampin 1990).

One of the reasons that effective media simulating flat parallel cracks are such an effective model for synthetic seismograms is that the wavelengths of seismic shear waves typically range from tens of metres to kilometres and are substantially greater than the dimensions of most cracks that are likely to cause the anisotropy (which probably range from a few microns to at most a few metres). This also implies that the elastic anisotropy causing the splitting is insensitive to the dimensions of the cracks. The elastic formulations of Hudson (1981) suggest that attenuation anisotropy is more sensitive to crack dimensions than elastic anisotropy, although up to the present time there is, to my knowledge,. only one observation of shear-wave attenuation anisotropy in crustal rocks that has been recognized (Liu *et al.* 1993a).

The distributions of cracks are also known to be fractal, both in sedimentary (Heffer & Bevan 1990; Yielding, Walsh & Watterson 1992) and igneous and metamorphic rocks (King 1983; Leary 1991; Leary & Abercrombie 1993). Fractal distributions of cracks have two important properties: first, cracks are scale invariant over a wide range of dimensions; and secondly, cracks tend to cluster in space. The scale invariance means that crack distributions contain cracks with a very wide range of dimensions, but because they cluster along the edges of lithologic units, there exist volumes of rock between the larger fractures which only contain cracks of comparatively small dimensions, the EDA cracks.

The reaction of seismic waves to distributions of fractures is determined by the relationship of the fracture dimensions to the seismic wavelengths. Thus, a fractal distribution is divided into two by the seismic wavelength. The reactions to small fractures can be modelled by effective media, whereas the reactions to larger fractures impose specific reflection, transmission, and diffraction effects. This division of the distribution into two will be accentuated by the tendency of small voids to be open and fluid-filled and hence compliant, whereas large fractures will tend to be closed by lithostatic pressure, and consequently less complaint. In addition, fluid-filled cracks with substantial impedance contrasts across the crack face are usually small, whereas large cracks are usually held closed and may be invisible to shear waves unless dilated by hydraulic pumping (Crampin & Booth 1989).

An example of a rock volume with no fractures larger than a metre is the granite batholith of the Underground Research Laboratory of the Atomic Energy of Canada, Ltd, at Pinawa, Manitoba, where there was a comprehensive examination of shear-wave splitting over a wide range of directions (Holmes *et al.* 1993). In the Mine-by experiment, the rock mass around an advancing test tunnel in a granite batholith, almost completely free of (macro) fractures, was sampled by 4200 Hz shear-wave signals excited on the walls of outer galleries, and recorded at three-component accelerometers in boreholes from the outer galleries, selected to give a good spatial sampling over a range of directions. The path lengths varied from about 7 m to 60 m, and the records displayed shear-wave splitting with observations covering almost 360" of azimuth and 180" of incidence angles. The polarizations match the theoretical polarizations expected of thin penny-shaped microcracks aligned perpendicular to the measured direction of minimum compressional stress some 20° from the vertical, broadly agreeing with the breakout notches in the tunnel itself.

Table 1 lists the percentages of differential shear-wave velocity anisotropy observed in igneous and metamorphic rocks measured (principally) above earthquakes. Differential shear-wave anisotropy is defined as SWA = $\{[\max (V_{S1}) - \min (V_{S2})]/ \max (V_{S1})\} \times 100$, where V_{S1} and V_{S2} are the velocities of the faster and slower split shear waves, respectively (Crampin 1989). Table 2 lists similar percentages in sedimentary basins from (principally) seismic-exploration investigations. Although neither table is a complete list of all observations, they are all reports known to the author, which provide sufficient information to identify the percentage of shear-wave velocity anisotropy. When only crack density ε is reported, $\varepsilon \times 100$ has been listed, since this is approximately equal to the percentage of differential shear-wave velocity anisotropy for crack densities less than about 0.1 when the V_P/V_S ratio is 1.732 (Crampin 1993a). In two cases, the percentage of shear-wave anisotropy has been inferred from observed P-wave anisotropy, assuming the anisotropy is caused by thin fluid-filled cracks when the differential shear-wave anisotropy is approximately twice the P-wave anisotropy (Crampin 1993a).

The frequencies of the shear waves displaying anisotropy in Tables 1 and 2 cover three orders of magnitude, ranging from about 5 Hz (Graham & Crampin 1993), with wavelengths of over 500 m, to 4200 Hz (Holmes *et al.* 1993), with wavelengths of about 80cm. The percentage of anisotropy appears to be independent of frequency, and frequencies are not listed in the tables.

Note that some publications, particularly in exploration seismology, list time delays as measures of anisotropy without giving path lengths or velocities, and it is not always possible to extract percentages of anisotropy or crack densities from the information provided. It would be useful if reports of shear-wave splitting invariably listed crack density, time delays, percentage anisotropy, shear-wave velocity, as well as depth range and the geology in which anisotropy is found.

3 OBSERVED ANISOTROPY IN INTACT SUBSURFACE ROCK

Tables 1 and 2 show the wide range of values of differential shear-wave velocity anisotropy observed in a wide range of geological and tectonic conditions. Percentages of anisotropy are listed in order of increasing anisotropy. In order to estimate the anisotropy of intact rock, I attempt to identify values measured near anomalous conditions, such as the

Table 1. Observed percentages of azimuthal differential shear-wave velocity anisotropy in (principally) igneous and metamorphic rocks. Sources of shear waves are earthquakes or natural events unless otherwise specified.

Percentage anisotropy	Depth range (km)	Rock type / comments	Location	Ref.
1.4‡$	c15	Volcanic rocks / aftershocks	Campi Flegrei, Italy	(1)
1.5	<17	Principally gabbro	Anza, CA, USA	(2)
2:o	<60	Above subduction zone	Wellington Peninsula, NZ	(3)
2.0, 2.5	<15	Mixed metam.& sedim. rocks	Los Angeles Basin, CA	(4)
2.3 ± 1.7	<3.5	Alternative interpret. to (2)	Anza, CA, USA	(5)
3.0*‡	<0.5	Welded fractured tuff	Tazawako, Akita, Japan	(6)
3.0@	Unspec.	Unspecified	Charlevoix Zone, Can.	(7)
3.5*	<0.45	Crystalline rock	Mojave Desert, CA, USA	(8)
<4.0	<5	Metamorphic rocks	W.Deep Levels, S.Africa	(9)
4.0*	0.4-0.5	Granite/shear-wave sources over 8m-60m raypaths	Manitoba, Canada	(10)
4.0	<15	Granite and mixed geology	Kinki, Honshu, Japan	(11)
4.0‡	<10	Volcanic rocks	Rift zone, Japan	(12)
4.3	<15	Mixed metam.& sedim. rocks	Los Angeles Basin, CA,	(4)
4.3‡	<10	Volcanic caldera	Long Valley, CA, USA	(13)
4.5	<12	Mixed metam.& sedim. rocks	TDP, Izmit, Turkey	(14)
4.5@	<10	Mixed metam.& sedim. rocks	Shikoku, Japan	(15)
5.0‡	<10	Volcanic rocks	E.Rift Zone, Hawaii	(16)
6.0©‡	<2	Volc.& sedim.rocks / geothermal area	Takinoue, Honshu, Japan	(17)
6.4‡	<10	Volcanic caldera	Long Valley, CA, USA	(18)
7.0‡	<3.1	Volcanic caldera	Phlegraean Fields, Italy	(16)
7.0$	<20	Metam.rocks / aftershocks	Nahami, NWT, Canada	(19)
8.00	<2	Granite / geothermal area	Cornwall, England	(20)
9.6‡	<10	Volc.cald. / resurgent dome	Long Valley, CA, USA	(18)
100	<30	Principally lower crust	TDP, Izmit, Turkey	(21)
10©	<15	Above subduction zone	Wellington Peninsula, NZ	(3)
10*+	<1	Granulite facies	Arunta Block, Australia	(22)
15‡†©	<10	Volc.caldera / fault zone	Long Valley, CA, USA	(23)
18‡©	<2	Volc.& sedim.rocks / geothermal area	Takinoue, Honshu, Japan	(17)

* shallow (uppermost 1 km);

$ aftershocks;

fault zone;

‡ volcanic rocks;

\+ inferred from observed P-wave velocity anisotropy;

© geothermal area of high heat flow;

@ estimated; essential information (usually *Vs*) omitted;

(1) Iannaccone & Deschamps (1989); (2) Peacock et *al.* (1988); (3) Gledhill (1991); (4) Du (1990); (5) Aster & Shearer (1991); (6) Kuwahara, Ito & Kiguchi (1991); (7) Buchbinder (1985); (8) Li, Leary & Aki (1990); (9) Graham, Crampin & Fernandez (1991); (10) Holmes, Crampin & Young (1993); (11) Kaneshima, Ando & Crampin (1987); (12) Kaneshima, Ito & Sugihara (1989); (13) Savage, Peppin & Vetter (1990); (14) Booth *et al.* (1985); (15) Kaneshima & Ando (1989); (16) Savage et *al.* (1989); (17) Kaneshima et al. (1988); (18) Shih & Meyer (1990); (19) Buchbinder (1990); (20) Roberts & Crampin (1986); (21) Graham & Crampin (1993); (22) Greenhalgh et al. (1990); (23) Savage, Peppin & Vetter (1990).

free surface, where larger crack densities and larger crack dimensions might be expected.

The uppermost 1 km of the crust typically has large percentages of anisotropy (marked with asterisks in Tables 1 and 2). Table 2, showing controlled-source measurements in sedimentary rocks where depth ranges are known, shows that particularly large anisotiopy is‘ 6ften found in very near-surface rocks (values in uppermost 60 m marked by double asterisks).

Other large percentages of anisotropy can be ascribed to anomalous regions, such as areas of recent deformation as, follows.

(1) ***Fault zones*** (Table 1: 15 per cent-Savage, Peppin &

Table 2. Observed percentages of azimuthal differential shear-wave velocity anisotropy in sedimentary rocks. Data from VSPs unless otherwise specified as: RFL-surface-to-surface reflection survey; RFR—surface-to-surface refraction survey; RVSP-reverse VSP; CHS-cross-hole survey; and EQ—earthquake sources.

Percentage anisotropy	Depth range (km)	Rock type / comments	Location	Ref.
0.7* - 3.8**	<0.47	Mixed sediments	Devine, TX, USA	(1)
1.4	<6.0	Unspec. sediments / RFL	Pennsylvania, USA	(2)
(1.5,2.0,2.5)©	<2.0	Mixed sediments / RFL	Dimmit, Zavala, and Frio Counties, TX,USA	(3)
1.4*	*co.9*	Clay, sandst.& limestone.	Caucasus Basin, Russia	(4)
1.6	1.1- 2.0	Shale & limestone	Paris Basin, France	*(5)*
1 .o-4.0	<2.4	Mixed sediments / RFL	Silo Field, WY, USA	(6)
-2.0	<3.0	Unspec.sediments / RFL	Unspecified, USA	*(7)*
2@	<2.6	Mixed sediments / RFL	Giddings Fld, TX, USA	(8)
2@	<6	Palaeozoic sedim / EQ	Enola, Arkansas, USA	(9)
2.4*	<1.1	Shale & limestone	Paris Basin, France	*(5)*
3.0*	*0.6* - 1.1	Shales & limestone	Paris Basin, France	(10)
(3.3, 4.0)*©, 7.0*	<1.0	Shales & carbonates	Romashkino, Russia	(11)
3.5±0.5	<3.0	Mixed sediments	Dilley, TX, USA	(12)
4*	<0.6	Unspecified sediments	CBTF, OK, USA	(13)
5.0**	<0.06	Bay Mud	San Franc.Bay, CA	*(14)*
7.0*@	<0.64	Unspecified sediments	Lost Hills Field, CA	(15)
>7.0‡©	*2.5*	Fractured chalk	Silo Field, WY, USA	(16)
(7.2 - 7.6)*†	<0.3	Fault zone	Oroville, CA, USA	(17)
8.0†	<1.4	Fault zone	Parkfield, CA, USA	(18)
9.0*	*co.4*	Unspecified sediments	Railroad Gap Field,CA	(19)
10*‡	0.8-0.85	Fractured sandstone	S.Casper Creek, WY	(20)
10.5**‡	<0.04	Clay & limestone / RVSP	CBTF, OK, USA	(21)
12**‡	<0.04	Clay & limestone / CHS	CBTF, OK, USA	(22)
12**	CO.04	Sandstone & clay	Livermore, CA, USA	(14)
14*	<0.47	Unspecified sediments	Cymric Field, CA,USA	(19)
>30**‡+	co.01	Limestone pavement / RFR	NW England, UK	(23)

* shallow (uppermost 1 km);

** very shallow (uppermost 60m);

† fault zone;

‡ specifically identified large fractures;

\+ inferred from observed P-wave velocity anisotropy;

© percentage anisotropy correlates with hydrocarbon production;

@ estimated; essential information (usually *Vs*) omitted;'

(1) Yardley & Crampin (1993); (2) Lynn & Thomsen (1990); (3) Li, Mueller & Crampin (1993); (4) Slater *et al.* (1993); (5) Bush & Crampin (1991); (6) Martin & Davies (1987); (7) Lynn & Thomsen (1986); (8) Mueller (1991); (9) Booth *et al.* (1990); (10) Lefeuvre, Cliet & Nicoletis (1989); (11) Cliet *et* al. (1991); (12) Alford (1986); (13) Queen & Rizer (1990); (14) Reported by Lynn (1991); (15) Winterstein & Meadows (1991a); (16) Lewis, Davis & Vuillermoz (1991); (17) Leary, Li & Aki (1987); (18) Daley & McEvilly (1990); (19) Winterstein & Meadows (1991b); (20) Shuck (1991); (21) Liu *et al.* (1993a); (22) Liu, Crampin & Queen (1991); (23) Crampin, McGonigle & Bamford (1980a).

Vetter 1990; Table 2: 7.2-7.6 per cent-Leary, Li & Aki 1978; 8 per cent-Daley & McEvilly 1990).

(2) Associated with aftershock sequences (Table 1: 7 per cent-Buchbinder 1990), although not all aftershock sequences yield high values (compare Table 1: 1.4 per cent-Iannaccone & Deschamps 1989).

(3) Areas where there has been hydraulic pumping, also associated with high heat flow (Table 1: 8 per cent-Roberts & Crampin 1986; 18 per cent-Kaneshima, Ito & Sugihara 1988).

(4) Specific intervals in fractured beds (Table 2: 7 per cent-Lewis *et al.* 1991; 10 per cent-Shuck 1991).

(5) Above subduction zones (Table 1: 10 per cent—Gledhill 1991) where active deformation and high pore-fluid pressures are expected (Prior & Behrmann 1990).

(6) Volcanic rocks associated with high heat flow (Table 1: 6 and 18 per cent-Kaneshima *et al.* 1968; 6.4 and 9.6 per cent-Shih & Meyer 1990; 7 per cent-Savage *et al.* 1989; 15 per cent-Savage *et al.* 1990). The 10 per cent of Graham & Crampin (1993), is confined principally to the lower crust,

and is also associated with volcanic rocks and high temperatures.

Excluding values identified as being associated with these special conditions, the range of anisotropy in Table 1 for what may be, considered as intact igneous and metamorphic rocks is 1.5 to 4.5 per cent, and the range for intact sedimentary rocks in Table 2 is 1.4 to 3.5 per cent with normalized (approximate) crack densities of $\varepsilon = 0.015$ to 0.045, and $\varepsilon = 0.014$ to 0.035, respectively.

The slightly lower maximum values of anisotropy for intact sedimentary rocks than for intact igneous and metamorphic rocks may have two causes: tectonic stability; and higher V_P/V_S ratios.

(1) Many measurements of anisotropy in sedimentary rocks are in stable sedimentary basins where active deformation is less pronounced [although changes due to the sinking or lowering of sedimentary basins may change pore-fluid pressures (Powley 1990) and modify crack densities], whereas measurements in igneous and metamorphic rocks are usually above earthquake sources, where the rocks may be expected to be more heavily deformed and fractured. None of the measurements in Table 2 is reported to be from over-pressurized reservoirs.

(2) The value of differential shear-wave anisotropy for a given crack density varies with the V_P/V_S ratio (Crampin 1993a). Thus a crack density of $\varepsilon = 0.05$ has differential shear-wave anisotropy of 5.5 per cent if V_P/V_S is 1.732 (Poisson's ratio of 0.25, which is frequently assumed for igneous and metamorphic rocks), 4.9 per cent anisotropy for V_P/V_S ratio of 2.5, and 4.6 per cent for V_P/V_S ratio of 3.5. We see that higher V_P/V_S ratios may account for a large part, but probably not all, of the lower range of percentages of anisotropy in intact sedimentary rocks.

Note that equating percentage anisotropy to ε x 100 introduces some bias into the estimates of crack density from velocity anisotropy for sedimentary rocks, because of the high V_P/V_S ratio in many sedimentary rocks, which has not been taken into account in obtaining Table 2. Note also that the equivalence of the percentage of differential shear-wave anisotropy to ε x 100 is a reasonable approximation for small crack densities (Crampin 1993a), but for crack densities greater than about $\varepsilon = 0.1$, displaying more than 10 per cent differential shear-wave anisotropy, there is no simple relationship between the degree of anisotropy and crack density.

4 EQUIVALENT CRACK DISTRIBUTIONS

The crack density $\varepsilon = Na^3/v$ can be normalized to $\varepsilon = a^3$, which represents a distribution of one crack of radius a in each unit cube in a regular distribution of equally sized circular cracks. Since, seismic-velocity anisotropy is insensitive to crack dimensions, as long as the crack size is substantially less than the seismic wavelength, the size of the cracks and the size of the unit cube is not specified. Table 3 lists equivalent values of normalized crack parameters for a range of crack densities giving a range of differential shear-wave anisotropies. Fig. 1 shows schematic illustrations of the density in terms of normalized crack dimensions assuming regular distributions of equally sized circular cracks for the five values of crack density in Table 3, ranging from lightly to heavily cracked rock. Note that it is difficult to accurately represent 3-D distributions in 2-D plane diagrams. The diagrams in Fig. 1 are not average cross-sections but represent the approximate separation of cracks in regular 3-D distributions of equally sized cracks at the relevant crack densities.

Table 3. Equivalent values of: (approximate) differential shear-wave velocity anisotropy, SWA; crack density, ε; and normalized crack radius, a.

SWA	1.5%	4.5%	10%	>10%	large
ε	0.015	0.045	0.10	0.125	0.42
a	0.25	0.33	0.46	0.50	0.75

Figure l(a) shows the equivalent crack distributions for a normalized crack density of $\varepsilon = 0.015$ displaying the 1.5 per cent minimum anisotropy observed along ray paths in igneous and metamorphic rocks, or strictly 1.4 per cent in sedimentary rocks (see Tables 1 and 2). Fig. l(b), for $\varepsilon = 0.045$ displaying 4.5 per cent anisotropy, appears to be the largest anisotropy observed in intact (unfractured) rock, excluding near-surface stress-release anomalies and the particular conditions cited in Section 3, above. The schematic diagrams Figs l(a) and l(b) display pervasive cracking, but there is still substantial intact matrix rock between the cracks. I suggest that values of crack density, $0.015 \leq \varepsilon \leq 0.045$, indicate the extent of the cracking in what would otherwise be thought of as intact rock, away from deformations associated with the stress release near the surface and other anomalous volumes within the rock mass.

Figures l(c), (d), and (e) show distributions for crack densities of $\varepsilon = 0.10$ and greater displaying 10 per cent and larger percentages of anisotropy. Such percentages are only found in rock in the uppermost 1 km, most frequently in the uppermost 60 m (Table 2), or in anomalous regions subsurface as specified in the previous section. The rock is substantially fractured: every crack in Fig. l(c) for $\varepsilon = 0.1$ is approximately a crack radius from about eight other cracks; Fig. l(d), where $\varepsilon = 0.125$ and the normalized crack diameter is unity, just spanning the unit cube, is shown for completeness; and Fig. l(c), for $\varepsilon = 0.42$, crack radius 0.75, shows a very heavily cracked rock.

Clearly, sections of cracks in crustal rocks seldom if ever look like the 2-D illustrations in Fig. 1, and several implicit assumptions have been made to obtain Table 3 and Fig. 1.

(1) It is assumed there are regular distributions of unconnected circular cracks of small, but not necessarily negligible aspect ratio, with dimensions much less than the seismic wavelengths sampling the rock. This may well be a reasonable approximation to the physical reality in uniform unfractured (intact) igneous and metamorphic rocks of low porosity and negligible permeability, as in the Mine-by experiment (Holmes *et al.* 1993). In sedimentary high-porosity rocks, however, where there is irregular intergranular pore space of significant porosity and permeability, the regular distributions in Fig. 1 are clearly not a good assumption. Nevertheless, shear-wave splitting with very similar characteristics is seen in both low- and high-porosity rocks (Tables 1 and 2; Crampin & Love11 1991), and there have been several examples of excellent matches of

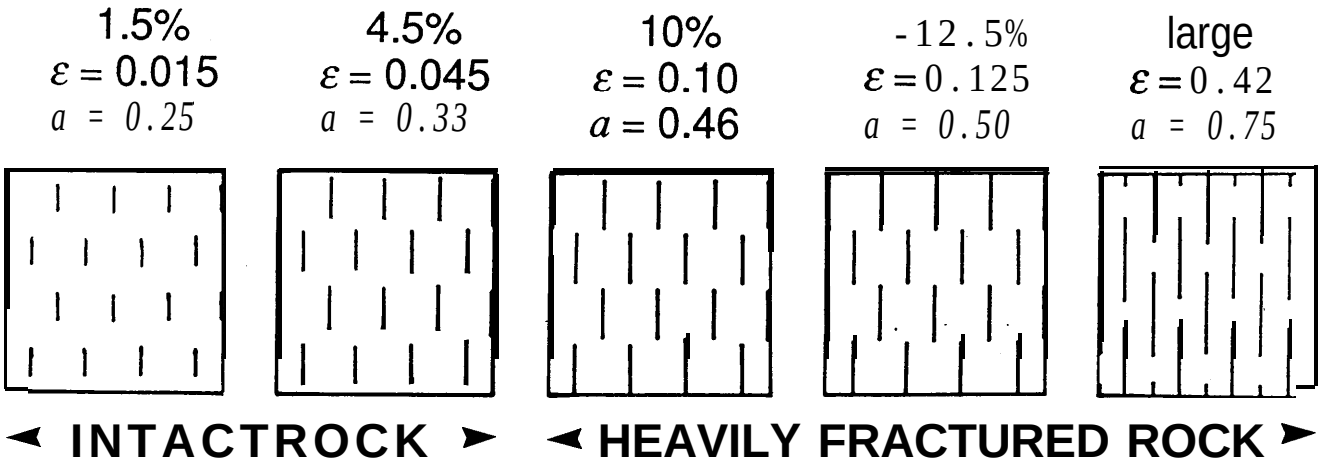

Figure 1. Schematic realization of percentage differential shear-wave velocity anisotropy in terms of crack density, ε; average normalized crack radius, a, for the values in Table 3. The panels represent approximate 2-D cross-sections through the cracked rocks.

full-waveform synthetic seismograms with recorded seismograms from ray paths in porous sedimentary sequences (Bush & Crampin 1991; Liu ***et al.*** 1993c; Slater ***et al.*** 1993; Yardley & Crampin 1990). These assume an equivalent cracked rock mass, using the Hudson (1980, 1981) formulations for small circular isolated parallel cracks. This suggests that the behaviour of seismic waves propagating through the preferentially aligned pore space in many sedimentary rocks can be simulated adequately by distributions of thin isolated cracks as illustrated in Fig. 1. It is assumed that one of the reasons for this is that seismic wavelengths are so much greater than the likely crack dimensions that the statistical averaging will be good, and it is suggested that the schematic illustrations of crack distributions in Fig. 1 give some indication of the relative degree of alignment even in sedimentary rocks.

(2) It is assumed that the cracks all have the same dimensions. This is clearly a strong assumption, but because of the good statistical sampling, the schematic illustrations of crack distributions in Fig. 1 are likely to give some indication of the relative degrees of cracking in real rocks.

(3) It is assumed that the cracks are uniformly aligned. There will certainly be a scatter about average (preferred) directions, however, Liu ***et al.*** (1993b) demonstrate that, to the first order, the crack density of a combination of parallel cracks with coplanar normals is the arithmetic sum of the cumulative crack densities and the polarization is the crack-density weighted mean of the individual polarizations. Consequently, if the scatter about a preferred direction relative to the stress orientations is comparatively small, as seems likely, the relationships suggested in Fig. 1 will be altered very little by a small range of crack orientations.

(4) Crack densities $\varepsilon \geq 0.1$ (more than 10 per cent shear-wave velocity anisotropy) can only exist if the fluid-pore pressure is sufficiently high to prop open cracks with substantial free faces. Cracks with pore pressures less than lithostatic pressure will tend to close, and closed cracks will tend to heal and become relatively transparent to shear-wave propagation. Large volumes of sedimentary strata with uniformly high pore-fluid pressures are known to exist in the over-pressurized fluid compartments (Powley 1990). High pore-fluid pressures are not as well known in igneous and metamorphic rocks as in sedimentary beds. This may be because there is less reason to sample rocks without hydrocarbons, and even in hydrocarbon reservoirs reliable pore-fluid pressures are difficult to obtain (Powley 1990). It is likely that the much lower overall porosity and lower overall permeability means that high pore-fluid pressures and large crack densities in most igneous and metamorphic rocks exist at least in localized volumes close to the source of the anomaly, such as the stress concentrations associated with fault zones, or in subduction zones where high pore-fluid pressures are known to exist (Prior & Behrmann 1990).

As a consequence of the division of observed values of anisotropy in Tables 1 and 2, I classify cracked rock into ***intact*** rock with less than about 4.5 per cent shear-wave anisotropy ($\varepsilon \leq 0.045$) and ***heavily fractured*** rock with more than 10 per cent anisotropy ($\varepsilon \geq 0.1$). It is convenient that the formulations of Hudson (1980, 1981) are valid for crack densities of up to about $\varepsilon = 0.1$, the range of crack densities for intact rock (Crampin 1984).

Rocks with shear-wave anisotropy of 10 per cent or greater ($\varepsilon \leq 0.1$) are so heavily fractured that any minor irregularity or disturbance will lead to through going fractures. In particular, the structure of the rock has so little shear strength that the cracked rock mass is unstable to small changes. Note that Hudson (1986) extended his earlier techniques to formally take account of crack-to-crack interactions, but these only make marginal differences to the elastic constants for crack densities less than about $\varepsilon = 0.1$, and in any case heavily fractured disaggregated rock cannot be modelled by effective medium constructs. Intact rock may have minor interconnections between individual cracks, but these will have negligible effects on Hudson's expressions for the long-wavelength limit and their effects on shear-wave propagation, and can be neglected.

5 FRACTURE CRITICALITY

There is, I suggest, a difference in kind between distributions of cracks in Figs l(a) and (b), and those in Figs l(c), (d), and (e). The average crack in Figs l(a) and (b)

may be considered to be surrounded by largely uncracked rock, whereas, as noted above, for the larger crack densities in Figs l(c), (d) and (e), an average crack is within a crack radius or less of an average of eight other cracks. Such rock is substantially fractured, as is confirmed by the observed anisotropy listed in Table 2, where larger percentages of anisotropy are only found comparatively near the surface, where stress relief can allow cracks and fractures to be significantly open, or where there are thought to be other known anomalies as listed in Section 3. The normalized crack radii between the minimum 1.5 per cent differential shear-wave anisotropy observed in most otherwise intact subsurface rocks, to the 10 per cent observed in rock near the surface, which is substantially fractured and unstable, differ by a factor less than two (0.46/0.25 = 1.84).

This is a remarkably small range of crack sizes for the large range of rock types sampled and large range of crack dimensions inferred from intact igneous rock (sub-millimetres to millimetres) to unstable fractured rock (metres to many metres). I suggest that this implies there is a value of crack density between $\varepsilon = 0.045$ and $\varepsilon = 0.1$ (normalized crack radii 0.33 and 0.46), between the representations in Figs l(b) and (c), which Crampin & Leary (1993) call ***fracture criticality,*** marking the transition from an essentially intact rock to unstable heavily fractured disaggregated rock. The range of normalized crack radii between intact and heavily fractured rock is extraordinarily small, 0.46/0.33 = 1.39. Thus, small increases in crack dimensions can critically alter the significance of the cracking. Any further deformation to the representation in Fig. l(b) would be likely to lead to pervasive cracking, where the cracks are likely to link up so there can be through-going fracturing, the dispersal of pore fluids through the enhanced permeability, and the loss of shear strength. The small fractures would tend to increase to larger fractures in a fractal relationship in the typical avalanching scenario associated with the phenomenon of self-organized criticality suggested by Bak & Tang (1989).

Once fracture criticality has been exceeded, pore fluids will tend to disperse with a consequent lowering of pore-fluid pressure. The lowering of pore pressure will allow cracks in the rock mass to close (and eventually heal) to crack densities below the level of fracture criticality. The presence of high pore-fluid pressures is expected to have a major effect on the behaviour at fracture criticality. The crack distributions in Figs l(c), (d) and (e) can only exist in a stable regime if the pore-fluid pressure is sufficient to keep the cracks propped open. This suggests that fracture criticality can only occur in the presence of pore-fluid pressures close to lithostatic pressure.

This suggests that pore-fluid seals have an important influence on the behaviour of rocks undergoing deformation. Thus, it might be expected that the over-pressurized fluid compartments suggested by Powley (1990), where fluid movement is contained by enclosing seals, would be particularly sensitive to changes in conditions acting on the rock mass.

A referee drew my attention to Peacock et al. (1994), published since this paper was submitted, who count crack densities up to 0.4 in cracked marble specimens which have not disintegrated. Photographs of the slides in which these cracks were made show an intersecting network of (randomly oriented) cracks surrounding almost every grain in the slides. This is typical of marble when heated (Rosengren & Jaeger 1968). In such rock fracture criticality has been exceeded, and Rosengren & Jaeger speak of such samples being 'crumbled with the fingers'. I suggest there are at least two reasons why the specimens have not disaggregated to individual grains. The cracking in the interior of the specimen may not extend to the surface, so that the cracked specimen is held together by a 'surface tension' of uncracked or less cracked rock. In addition, the photographs show a minutely irregular interlocking jigsaw-like network of cracks that would not easily pull apart. The 3-D jigsaw of grains is probably the reason that marble shows a gradual rollover above yield strength rather than the brittle failure typical of most rocks (Fredrich, Evans & Wong 1989).

There are also difficulties in the definition of crack density for large values of randomly oriented cracks. The expression for crack density, $\varepsilon = na^3/v$, usually refers to weak distributions of flat or nearly flat (strictly elliptical) non-intersecting cracks. Fig. 1 suggests that this definition should to be confined to values of ε less than about $\varepsilon = 0.1$. I suggest it may be reasonable to extend the definition to stronger distributions of parallel non-intersecting cracks as in this paper, which 'in any case does not rely on any quantitative evaluation above $\varepsilon = 0.1$, but there are problems in using this definition for larger crack densities when the cracks intersect. Fig. 1 shows that for crack densities above a value of $\varepsilon = 0.1$, where each crack spans a unit cube, randomly oriented cracks necessarily intersect and the definition for crack density breaks down as the number of cracks is then indeterminate.

6 DISCUSSION

Observations of shear-wave splitting demonstrate that the range of differential shear-wave velocity anisotropy from intact ostensibly unfractured subsurface rock to heavily fractured rock is equivalent to an extraordinarily small range of normalized crack dimensions-compare Figs l(b) and (c). The behaviour appears to be similar in all rocks traversed by shear waves despite the wide range of porosity, permeability, and internal structure in sedimentary, igneous, and metamorphic rocks. It is argued that this implies that most crustal rocks are so pervaded by fluid-filled cracks that they are close to fracture criticality: the level of cracking marking the transition from what would be thought of as coherent unfractured rock to an unstable disaggregated heavily fractured rock mass. The actual level for fracture criticality would depend on details of pore-fluid pressures and rock type, and geological conditions.

Once fracture criticality has been reached, average cracks would be within a crack radius or less of at least eight other cracks. With such closely spaced cracks, the structure would be weak, and the proximity to this state of fracture criticality implies that most rocks are compliant, where small deformations or changes of conditions may have major effects on the behaviour of the rock mass. Since shear-wave splitting is very sensitive to this internal geometry of the aligned cracks along the ray path, shear waves can be used to monitor the detailed changes to the rock mass.

The results presented here show that some measure of the

proximity to fracture criticality can be estimated from monitoring shear-wave splitting in the rock mass. This means that any situation, where conditions acting on the rock mass change and modify the internal geometry of distributions of cracks in the rock, may be monitored by analysing shear-wave splitting. Since the transition to fracture criticality is likely to be crucial for many processes in the rock mass, and ability to monitor the transition by analysing shear waves may have several applications.

(1) Reservoirs close to fracture criticality are likely to display increased hydrocarbon permeability allowing pore fluids to disperse more easily and thus permit higher rates of production. (Such enhanced permeability is expected to vary with direction and be anisotropic, perhaps strongly anisotropic, which may mean that the behaviour needs to be closely controlled for the full benefits of enhanced permeability to be attained.) There have been several cases reported where the degree of shear-wave anisotropy have been correlated with hydrocarbon production (Cliet et *al.* 1991; Li et *al.* 1993), as well cases where higher production has been specifically associated with the presence of large fractures (Mueller 1991; Lewis *et al.* 1991).

The compliant nature of the rock mass, where small changes in conditions may lead to substantial changes in the behaviour of the rock mass, opens many possibilities. Any situation where rocks are stressed, strained, or otherwise deformed, will modify the internal crack geometry without necessarily leading to fracture criticality, but may still be monitored by analysing shear-wave splitting.

(2) Over-pressurized reservoirs, with fracture criticality and enhanced permeability, are optimum conditions for hydrocarbon production. However, as production proceeds, pore-fluid pressure would decrease locally around the production well and the crack density within that volume would contract to below fracture criticality with the consequent loss of permeability and decline in production probably by encouraging adverse fingering. Consequently, it is desirable to maintain fluid-pore pressures in order to maintain enhanced permeability and enhanced levels of production. These ideas may not be new, but the importance of the results presented here is that the recognition that the proximity of fracture criticality and enhanced permeability can be monitored by analysing shear-wave splitting. This opens the possibility of monitoring and possibly even controlling enhanced oil-recovery operations so as to maximize recovery.

(3) The effects of hydraulic fracturing may be predicted and evaluated by analysing shear-wave splitting. Crampin & Booth (1989) identified changes in orientation of shear-wave polarizations induced by hydraulic pumping in a granite batholith.

(4) Changes of stress and strain before earthquakes would be expected to modify crack geometry and change the behaviour of shear-wave splitting. Changes in shear-wave splitting were identified by Peacock et al. (1988) before the North Palm Springs $M = 6$ earthquake, which were later confirmed by Crampin *et* al. (1990, 1991). Similar changes have also been reported in less-controlled observations before smaller earthquakes by Booth *et al.* (1990) and Liu et *al.* (1993c). These changes could be interpreted as increases in crack aspect ratio (dilatancy) as the stress increases before earthquakes and a decrease in aspect ratio at the time, or in one case (Booth et *al.* 1990), shortly before the earthquake.

(5) Other sources of seismic anisotropy, such as crystals, may exhibit quite large percentages of shear-wave velocity anisotropy. The demonstration that consistently, almost all examples of percentages greater than about 4.5 per cent, can be associated with rock where heavy fracturing is either directly observed or expected, is further confirmation that the almost universally observed shear-wave splitting in crustal rocks is caused principally by aligned cracks, microcracks, and preferentially oriented pore space.

ACKNOWLEDGMENTS

I thank Peter Leary, Enru Liu and Sergey Zatsepin for many illuminating discussions about crack distributions. This work was partially supported by the Sponsors of the Edinburgh Anisotropy Project, and partially by the Natural Environment Research Council, and is published with the approval of the EAP Sponsors, and the Director of the British Geological Survey (NERC) .

REFERENCES

Alford, R.M., 1986. Shear data in the presence of azimuthal anisotropy: Dilley, Texas, *56th Ann. Int. SEG Meeting, Houston, Expanded Abstracts, 476-479.*

Aster, R.C. & Shearer, P.M., 1991. High-frequency borehole seismograms recorded in the San Jacinto fault zone, Southern California, Bull. *seism. Soc. Am.,* **81,** 1057-1080.

Bak, P. & Tang, C., 1989. Earthquakes as a self-organized critical phenomenon, *J. geophys. Res.,* **94, 15** 635-15 637.

Booth, D.C. & Crampin, S., 1985. Shear-wave polarizations on a curved wavefront at an isotropic free-surface, *Geophys. J. R. astr. Soc., 83,* 31-45.

Booth, D.C., Crampin, S., Evans, R. & Roberts, G., 1985. Shear-wave polarizations near the North Anatolian Fault-I. Evidence for anisotropy-induced shear-wave splitting, *Geophys. J. R. astr. Soc.,* **83,** 61–73.

Booth, D.C., Crampin, S., Lovell, J.H. & Chiu, J.-M., 1990. Temporal changes in shear wave splitting during an earthquake swarm in Arkansas, *J. geophys. Res.,* 95, 11 151-11 164.

Bregman, N.D., 1989. Seismic tomography at a fire-flood site, *Geophysics,* **54,** 1082-1090.

Buchbinder, G.G., 1985. Shear-wave splitting and anisotropy in the Charlevoix seismic zone, Quebec, *Geophys. Res. Lett.,* **12,** 425-428.

Buchbinder, G.G., 1990. Shear wave splitting and anisotropy from the aftershocks of the Nahanni, Northwest Territories, earthquakes, *J. geophys. Res., 95, 4777-4785.*

Bush, I. & Crampin, S., 1991. Paris Basin VSPs: case history establishing combinations of matrix- and crack-anisotropy from modelling shear wavefields near point singularities, *Geophys. J. Int.,* **107, 433-447.**

Cliet, C., Brodov, L., Tikhonov, A., Marin, D. & Michon, D., 1991. Anisotropy survey for reservoir definition, *Geophys. J. Znt.,* **107, 417-427.**

Crampin, S., 1978. Seismic wave propagation through a cracked solid: polarization as a possible dilatancy diagnostic, *Geophys. J. R. astr. Soc., 53, 467-496.*

Crampin, S., 1981. A review of wave motion in anisotropic and cracked elastic-media, *Wave Motion, 3,* 343-391.

Crampin, S., 1984. Effective anisotropic elastic-constants for wave propagation through cracked solids, *Geophys. J. R. astr. Soc.,* 76, 135-145.

Crampin, S., 1989. Suggestions for a consistent terminology for seismic anisotropy, ***Geophys. Prosp.*, 37,** 753–770.

Crampin, S., 1993a. A review of the effects of crack geometry on wave propagation through aligned cracks, ***Can. J. expl. Geophys., 29,*** 3-17.

Crampin, S., 1993b. Arguments for EDA, ***Can. J. expl. Geophys.,*** 29, 18-30.

Crampin, S. & Booth, D.C., 1989. Shear-wave splitting showing hydraulic dilatation of pre-existing joints in granite, ***Sci. Drill., 1, 21-26.***

Crampin, S. & Evans, R., 1986. Neotectonics of the Marmara Sea region of Turkey, ***J. geol. Soc.*, 143, *343-348.***

Crampin, S. & Leary, P., 1993. Limits to crack density: the state of fractures in crustal rocks, ***63rd Ann. Int. SEG Meeting, Washington, Expanded Abstracts,*** 758-761.

Crampin, S. & Lovell, J.H., 1991. A decade of shear-wave splitting in the Earth's crust: what does it mean? what use can we make of it? and what should we do next?, ***Geophys. J. Int.*, 107,** 387-407.

Crampin, S., Evans, R. & Atkinson, B.K., 1984. Earthquake prediction: a new physical basis, ***Geophys. J. R. astr. Soc., 76,*** 147-156.

Crampin, S., McGonigle, R. & Bamford, D., 1980a. Estimating crack parameters from observations of P-wave velocity anisotropy, ***Geophysics, 45, 345-360.***

Crampin, S., Evans, R., Üçer, B., Doyle, M., Davis, J.P., Yegorkina, G.V. & Miller, M., 1980b. Observations of dilatancy-induced polarization anomalies and earthquake prediction, ***Nature, 286, 874-877.***

Crampin, S., Bush, I., Naville, C. & Taylor, D.B., 1986. Estimating the internal structure of reservoirs with shear-wave VSPs, ***The Leading Edge, 5,*** 11, 35-39.

Crampin, S., Booth, D.C., Evans, R., Peacock, S. & Fletcher, J.B., 1990. Changes in shear wave splitting at Anza near the time of the North Palm Springs Earthquake, ***J. geophys. Res.,*** 95, 11197-11212.

Crampin, S., Booth, D.C., Evans, R. Peacock, S. & Fletcher, J.B., 1991. Comment on 'Quantitative Measurements of Shear Wave Polarizations at the Anza Seismic Network, Southern California: Implications for Shear Wave Splitting and Earthquake Prediction' by R. C. Aster, P. M. Shearer & J. Berger, ***J. geophys. Res., %,*** 6403-6414.

Daley, T.M. & McEvilly, T.V., 1990. Shear-wave anisotropy in the Parkfield Varian Well VSP, ***Bull. seism. Soc. Am., 80, 857-869.***

De Buyl, M., 1989. Optimal field development with seismic reflection data, ***The Leading Edge, 8, 4,*** 14-19.

Du, X., 1990. On shear-wave splitting in the Los Angeles basin, ***Pure. appl. Geophys., 134,*** 175-194.

Fredrich, J.T., Evans, B. & Wong, T.-F., 1989. Micromechanics of the brittle to plastic transition on Carrara Marble, ***J. geophys. Res., 94,*** 4129–4145.

Gledhill, K.R., 1991. Evidence for shallow and pervasive seismic anisotropy in the Wellington Region, New Zealand, ***J. geophys. Res., 96,*** 21503-21516.

Graham, G. & Crampin, S. 1993. Shear-wave splitting from regional earthquakes in Turkey, ***Can. J. expl. Geophys., 29,*** 371-379.

Graham, G., Crampin, S. & Fernandez, L.M., 1991. Observations of shear-wave polarizations from rockbursts in a South African gold field: and analysis of acceleration and velocity recordings. ***Geophys. J. Int., 107, 661-672.***

Greaves, R.J. & Fulp, T.J., 1987. Three-dimensional seismic monitoring of an enhanced oil recovery process, ***Geophysics,*** 52, 1175-l 187.

Greenhalgh, S.A., Wright, C., Goleby, B. & Soleman, S., 1990. Seismic anisotropy in granulite facies rocks of the Arunta Block, Central Australia, ***Geophys. Res. Lett.,*** 17, 1513-1516.

Heffer, K.J. & Bevan, T.G., 1990. Scaling relationships in natural fractures, ***Europe 90, The Hague, 1990, Soc.*** Pet. ***Eng. paper*** 20981.

Holmes, G.M., Crampin, S. & Young, R.P., 1993. Preliminary analysis of shear-wave splitting in granite at the Underground Research Laboratory, Manitoba, ***Can. J. expl. Geophys., 29,*** 140-152.

Hudson, J.A., 1980. Overall properties of a cracked solid, ***Math. Proc. Camb. phil. Soc., 88,*** 371-384.

Hudson, J.A., 1981. Wave speeds and attenuation of elastic waves in material containing cracks, ***Geophys, J. R. astr. Soc., 64,*** 133-150.

Hudson, J.A., 1986. A higher order approximation to the wave propagation constants for a cracked solid, ***Geophys. J. R. astr. Soc.***, 87, 265-274.

Iannaccone, G. & Deschamps, A., 1989. Evidence of shear-wave anisotropy in the upper crust of Central Italy, ***Bull. seism. Soc. Am.,*** 79, 1905-1912.

Kaneshima, S., 1990. Origin of crustal anisotropy: shear wave splitting studies in Japan, ***J. geophys. Res.,*** 95, 11 121-11 133.

Kaneshima, S. & Ando, M., 1989. An analysis of split shear waves observed above crustal and uppermost mantle earthquakes beneath Shikoku, Japan, implications in effective depth extent of seismic anisotropy, ***J. geophys. Res., 94,*** 14 077-14 092.

Kaneshima, S., Ando, M. & Crampin, S., 1987. Shear-wave splitting above small earthquakes in the Kinki District of Japan, ***Phys. Earth. planet. Inter., 45, 45-58.***

Kaneshima, S., Ito, H. & Sugihara, M., 1988. Shear-wave splitting observed above small earthquakes in a geothermal area of Japan, ***Geophys. J. R. astr Soc., 94,*** 399-411.

Kaneshima, S., Ito, H. & Sugihara, M., 1989. Shear wave polarization anisotropy observed in a rift zone in Japan, ***Tectonophysics,*** 157, 281-300.

King, G., 1983. The accommodation of large strains in the upper lithosphere of the Earth and other solids by self-similar fault systems: the geometrical origin of b-value, ***Pure. appl. Geophys., 121,*** 761-815.

Kuwahara, Y., Ito, H. & Kiguchi, T., 1991. Comparison between natural fractures and fracture parameters derived from VSP, ***Geophys. J. Int., 107, 475-483.***

Leary, P., 1991. Deep borehole evidence for fractal distribution of fractures in crystalline rock, ***Geophys. J. Int., 107, 615-627.***

Leary, P.C. & Abercrombie, R., 1993. Fractal fracture scattering origin of S-wave coda: spectral evidence from recordings at ***2.5*** km, ***Geophys. Res. Lett.,*** in press.

Leary, P.C., Li, Y.-G. & Aki, K., 1987. Observation and modeling of fault-zone fracture seismic anisotropy-I. ***P, SV*** and ***SH*** travel times, ***Geophys. J. R. astr. Soc., 91, 461-484.***

Lefeuvre, F., Cliet, C. & Nicoletis, L., 1989. Shear-wave birefringence measurement and detection in the Paris basin, ***59th Ann. Int. SEG Meeting, Dallas, Expanded Abstracts, 2, 786-790.***

Lefeuvre, F., Turpening, R., Caravana, C., Born, A. & Nicoletis, L., 1993. Vertical open fractures and shear-wave velocities derived from VSPs, full waveform acoustic logs, and televiewer data, ***Geophysics, 56,*** 818-834.

Lewis, C., Davis, T.L. & Vuillermoz, C., 1991. Three-dimensional multicomponent imaging of reservoir heterogeneity, Silo Field, Wyoming, ***Geophysics, 56,*** 2048–2056.

Li, Y.-G., Leary, P.C. & Aki, K., 1990. Ray series modelling of seismic wave travel times and amplitudes in three-dimensional heterogeneous anisotropic crystalline rock: borehole vertical seismic profiling seismograms from the Mojave Desert, California, ***J. geophys. Res., 95,*** 11225-11239.

Li, X.-Y., Mueller, M.C. & Crampin, S., 1993. Case studies of shear-wave splitting in reflection surveys in South Texas, ***Can. J. expl. Geophys., 29,*** 189-215.

Liu, E., Crampin, S. & Queen, J.H., 1991. Fracture detection using

crosshole surveys and reverse vertical seismic profiles at the Conoco Borehole Test Facility, Oklahoma, *Geophys. J. Int.*, **107,** 449–463.

Liu, E., Crampin, S., Queen, J.H. & Rizer, W.D., 1993a. Velocity and attenuation anisotropy caused by microcracks and macrofractures in azimuthal reverse VSPs, *Can. J. expl. Geophys., 29,* 177-188.

Liu, E., Crampin, S. Queen, J.H. & Rizer, W.D., 1993b. Behaviour of shear waves in rocks with two sets of parallel cracks, *Geophys. J. Int.,* **113, 509-517.**

Liu, Y., Booth, D .C., Crampin, S., Evans, R. & Leary, P., 1993c. Possible temporal variations in shear-wave splitting at Parkfield, *Can. J. expl. Geophys., 29, 380-390.*

Lüschen, E., Söllner, W., Hohrath, A. & Rabbel, W., 1991. Integrated *P-* and S-wave borehole experiments at the KTB-Deep Drilling Site in the Oberpfalz area (SE Germany), in *Continental Lithosphere: Deep Seismic Reflections, Geodynamics, 22,* 121-133.

Lynn, H.B., 1991. Field measurements of azimuthal anisotropy: first 60 metres, San Francisco Bay area, CA, and estimation of the horizontal stresses' ratio from V_{S1}/V_{s2}, *Geophysics, 56,* 822-832.

Lynn, H.B. & Thomsen, L.A., 1986. Reflection shear-wave data along the principal axes of azimuthal anisotropy, *56th Ann. Int. SEG Meeting, Houston, Expanded Abstracts, 473-476.*

Lynn, H.B. & Thomsen, L.A., 1990. Reflection shear-wave data collected near the principal axes of azimuthal anisotropy, *Geophysics, 55,* 147-156.

Martin, M.A. & Davies, T.L., 1987. A new tool for evaluating fractured reservoirs, *The Leading Edge, 6, 6, 22-28.*

Mueller, M.C., 1991. Prediction of lateral variability in fracture intensity using multicomponent shear-wave surface seismic as a precursor to horizontal drilling in Austin Chalk, *Geophys. J. Int.*, **107, 409-415.**

O'Connell, R.J. & Budiansky, B., 1974. Seismic velocities in dry and saturated cracked solids, *J. geophys. Res., 79,* 5412-5426.

Peacock, S., Crampin, S., Booth, D.C. & Fletcher, J.B., 1988. Shear-wave splitting in the Anza seismic gap, Southern California: temporal varitions as possible precursors, *J. geophys. Res., 93, 3339-3356.*

Peacock, S., McCann, C., Sothcott, J. & Astin, T.R., 1994. Seismic velocities in fractured rocks: an experimental verification of Hudson's theory, *Geophys. Prosp., 42, 27-80.*

Prior, D.J. & Behrmann, J.H., 1990. Thrust-related mudstone fabrics from the Barbados forearc: a backscattered scanning electron microscope study, *J. geophys. Res., 95,* 9055–9067.

Powley, D.E., 1990. Pressures and hydrogeology in petroleum basins, *Earth Sci. Rev., 29,* 215-226.

Queen, J.H. & Rizer, W.D., 1990. An integrated study of seismic anisotropy and the natural fracture system at the Conoco Borehole Test Facility, Kay County, Oklahoma, *J. geophys. Res., 95,* 11255-11273.

Roberts, G. & Crampin, S., 1986. Shear-wave polarizations in a Hot-Dry-Rock geothermal reservoir: anisotropic effects of fractures, *Int. J. Rock Mech. Min. Sci., 23,* 291-302.

Robertson, J.D., 1989. Reservoir management using 3-D seismic data, *The Leading Edge, 8, 2, 25-31.*

Rosengren, K.J. & Jaeger, J.C., 1968. The mechanical properties of an interlocked low-porosity aggregate, *Geotechnique,* **18,** 317-326.

Savage, M.K., Peppin, W.A. & Vetter, U.R., 1990. Shear-wave anisotropy and stress direction in and near Long Valley Caldera, California, 1979-1988, *J. geophys. Res., 95,* 11 165-11 177.

Savage, M.K., Shih, X.R., Meyer, R.P. & Aster, R.C., 1989. Shear-wave anisotropy of active tectonic regions via automated S-wave polarization analysis, *Tectonophysics,* **165, 279-292.**

Shih, X.R. & Meyer, R.P., 1990. Observation of shear wave splitting from natural events: South Moat of Long Valley Caldera, California, June 29 to August 12, 1982, *J. geophys. Res.,* 95, 11 179-11 195.

Shuck, E.L., 1991. Azimuthal anisotropy analysis from shear VSPs, *Geophys. J. Int.*, **107, 639-647.**

Slater, C., Crampin, S., Brodov, L.Y. & Kuznetsov, V.M., 1993. Observations of anisotropic cusps in transversely isotropic clay, *Can. J. expl. Geophys., 29,* 216-226.

Stoneley, R., 1955. The propagation of surface elastic waves in a cubic crystal, *Proc. R. Soc.*, A, 232, 447-458.

Stoneley, R., 1963. The propagation of surface waves in an elastic medium with orthorhombic symmetry, *Geophys. J. R. astr. Soc.*, 8, 176-186.

Winterstein, D.F. & Meadows, M.A., 1991a. Shear-wave polarization and subsurface stress directions at Lost Hills field, *Geophysics,* 56, 1331-1348.

Winterstein, D.F. & Meadows, M.A., 1991b. Changes in shear-wave polarization azimuth with depth in Cymric and Railroad Gap oil fields, *Geophysics, 56,* 1349-1364.

Yardley, G. & Crampin, S., 1990. Automatic determination of anisotropic parameters from shear-wave splitting in the Lost Hills VSP, *60th Ann. Int. SEG Meeting, San Francisco, Expanded Abstracts, 2,* 1424-1426.

Yardley, G.S. & Crampin, S., 1993. Shear-wave anisotropy in the Austin Chalk, Texas, from multi-offset VSP data: case studies, *Can. J. expl. Geophys., 29,* 163-176.

Yielding, G., Walsh, J. & Watterson, J., 1992. The prediction of small-scale faulting in reservoirs, *First Break,* **10, 449-460.**